# Chest Imaging

Ruth G. Keijsers, MD, PhD[a], Marcel Veltkamp, MD, PhD[b], Jan C. Grutters, MD, PhD[b,c,*]

**KEYWORDS**

• Sarcoidosis • Chest radiography • HRCT • FDG PET/CT • Disease activity

**KEY POINTS**

- Staging pulmonary sarcoidosis has been performed using the chest radiograph Scadding criteria for more than 50 years.
- High-resolution computed tomography (HRCT) is an essential diagnostic modality in diagnosing sarcoidosis.
- Pulmonary sarcoidosis is notorious for mimicking many other interstitial lung diseases.
- Fluorodeoxyglucose F 18 (FDG) PET/computed tomography (CT) is able to image active sarcoidosis in mediastinal and hilar lymph nodes, lung parenchyma, and myocardium.
- FDG PET/CT can be used to evaluate sarcoidosis activity in patients with persistent symptoms, stage IV disease, and cardiac sarcoidosis and for treatment monitoring.
- Diffuse lung parenchymal activity in FDG PET/CT is associated with loss of pulmonary function after 1 year when untreated. In addition, a decrease in lung parenchymal FDG uptake correlates with lung functional improvement on immunosuppressive treatment.

## INTRODUCTION

The clinical manifestations of sarcoidosis are highly variable and often nonspecific. Every organ can be affected, but thoracic involvement occurs in more than 90% of patients.[1] For pulmonary sarcoidosis, therefore, chest imaging by chest radiograph or HRCT, is important for diagnosing and management of this disease. In sarcoidosis patients with extrapulmonary manifestations, such as cardiac sarcoidosis or neurosarcoidosis, other imaging modalities are warranted. In these patients MRI and FDG-PET scanning are increasingly recognized as essential imaging techniques required for adequate diagnosing sarcoidosis localization and disease management.[2] The first publications on radiological findings on sarcoidosis date from the early twentieth century.[3] More than 50 years ago, Professor John Guyett Scadding proposed 5 stages of disease based on chest radiographs.[4] In the past decades, multiple scoring systems for sarcoidosis have been developed, but the Scadding stages still are the most used in clinical practice.[5,6]

## RADIOGRAPHIC SCORING SYSTEMS: SCADDING STAGING

Sarcoidosis is commonly staged according to its appearance on the chest radiograph following the Scadding criteria (**Table 1**).[4] Stage 0 indicates no visible intrathoracic findings. Stage I represents bilateral hilar lymphadenopathy, which may be accompanied by paratracheal lymphadenopathy.

Disclosures: None.

[a] Department of Nuclear Medicine, St. Antonius Hospital, Koekoekslaan 1, Utrecht, Nieuwegein 3435 CM, The Netherlands; [b] ILD Center of Excellence, St. Antonius Hospital, Koekoekslaan 1, Utrecht, Nieuwegein 3435 CM, The Netherlands; [c] Division of Heart and Lungs, University Medical Center, Utrecht, The Netherlands
* Corresponding author. ILD Center of Excellence, St. Antonius Hospital, Koekoekslaan 1, Utrecht, Nieuwegein 3435 CM, The Netherlands.
*E-mail address:* j.grutters@antoniusziekenhuis.nl

Clin Chest Med 36 (2015) 603–619
http://dx.doi.org/10.1016/j.ccm.2015.08.004
0272-5231/15/$ – see front matter 

**Table 1**
**Radiographic staging of sarcoidosis patients at presentation according to the Scadding criteria**

| Radiographic Stage | Chest Radiograph | Frequency (%) | Resolution (%) |
|---|---|---|---|
| 0 | Normal | 5–15 | |
| I | BHL | 25–65 | 60–90 |
| II | BHL and pulmonary infiltrates | 20–40 | 40–70 |
| III | Pulmonary infiltrates without BHL | 10–15 | 10–20 |
| IV | Advanced pulmonary fibrosis | 5 | 0 |

The estimated frequency at presentation is given as well as the probability of spontaneous resolution during disease course.
*Abbreviation:* BHL, bilateral hilar lymphadenopathy.

Stage II represents bilateral hilar lymphadenopathy accompanied by parenchymal infiltration. Stage III represents parenchymal infiltration without hilar lymphadenopathy. Stage IV consists of advanced fibrosis with evidence of honeycombing, hilar retraction, bullae, cysts, and emphysema. Despite the nomenclature, patients do not all progress through stages I to IV and these stages have no sequential order. For example, a patient may present with stage III that normalizes during follow-up. Also, it can be seen that a patient who initially presents with stage I disease that normalizes can present later with parenchymal disease only (stage III).[7] Hillerdal and colleagues[8] found that in a cohort of patients presenting with stage I disease, 9% progressed to stage II compared with 1.6% who progressed to stage III or IV. Of patients presenting with stage II disease, only 5.5% progressed to stage III or IV disease.

An interesting feature of the Scadding criteria is that they give prognostic information.[9–11] In stage I disease, spontaneous resolution occurs in 60% to 90% of patients. Spontaneous resolution occurs in 40% to 70% of patients with stage II disease and in 10% to 20% of patients with stage III disease. A majority of spontaneous remissions occur within the first 2 years of disease presentation. There is no spontaneous resolution in patients with stage IV pulmonary sarcoidosis. An important limitation of the Scadding criteria is the great interobserver variability, especially between stages II and III and between stages III and IV.[7] Furthermore, stage IV fibrotic sarcoidosis does not always indicate end-stage disease. It has been demonstrated that in 50% of patients with stage IV pulmonary sarcoidosis, metabolic activity is present on FDG PET/CT.

## LARGE AIRWAY INVOLVEMENT

Sarcoidosis of the upper respiratory tract may involve the nose, sinuses, larynx, oral cavity, ear, trachea, and bronchi.[12,13] The incidence of sarcoidosis of the upper respiratory tract is approximately 5%.[14] During bronchoscopy, common lesions in the trachea as well as in the bronchi are erythema, thickening of the mucosa, and a cobblestone appearance (**Fig. 1**), which yields a high number of granulomas on biopsy. A small study by Shorr and colleagues[15] showed that 71% of sarcoidosis patients undergoing bronchoscopy had bronchial abnormalities. Severe endoluminal stenosis of the trachea or main bronchi is rare in sarcoidosis, estimated as less than 1%.[16] When diagnosing sarcoidosis, even in patients with a normal-appearing airway, granulomas can be identified in approximately 30% of patients.[15]

## MEDIASTINAL AND HILAR LYMPHADENOPATHY

Lymphadenopathy is the most common intrathoracic manifestation of sarcoidosis, occurring in approximately 80% of patients during their illness,


**Fig. 1.** Endobronchial cobblestone appearance in a 57-year-old sarcoidosis patient. Biopsy-proved multiple non-necrotizing granulomas.

irrespective of radiographic staging.[17–23] An overview of common and uncommon sites of thoracic lymphadenopathy in sarcoidosis is given in **Box 1**. In most cases, bilateral hilar lymphadenopathy is present (**Fig. 2**), with unilateral hilar adenopathy occurring in only 3% to 5% of patients.[17,24,25] When present, unilateral hilar lymphadenopathy is more common on the right side than on the left side. Furthermore, besides the hilar region, lymphadenopathy in sarcoidosis is also seen in the right paratracheal, aortopulmonary window, and tracheobronchial regions.[20–23,26] A typical example of bilateral lymphadenopathy and right paratracheal lymphnode enlargement in sarcoidosis is known as Garland triad or 1-2-3 sign.

**Box 1**
**Classical versus more uncommon features of pulmonary sarcoidosis seen on HRCT**

*Classic findings, potentially reversible*

Lymphadenopathy: bilateral hilar, mediastinal, right paratracheal, subcarinal, aortopulmonary

Reticulonodular pattern: micronodules (2–4 mm, well defined, bilateral distribution)

Perilymphatic distribution of nodules (peribronchovascular, subpleural, interlobular septal)

Predominant upper and middle zones parenchymal abnormalities

*Uncommon findings, potentially reversible*

Lymphadenopathy: unilateral, isolated, anterior and posterior mediastinal, paracardiac

Reticular pattern

Isolated cavitations

Isolated ground glass opacities without micronodules

Mosaic attenuation pattern

Pleural disease (effusion, pleural thickening, chylothorax, pneumothorax)

Mycetoma

Macronodules (>5 mm, coalescing); galaxy sign and cluster sign

*Classic findings reflecting irreversible fibrosis or chronic disease*

Reticular opacities, predominantly middle and upper zones

Architectural distortion

Traction bronchiectasis

Volume loss, predominantly upper lobes

Calcified lymphnodes

Fibrocystic changes

*Uncommon findings reflecting irreversible fibrosis or chronic disease*

Honeycomb-like changes

Reticular opacities in predominantly lower lobes

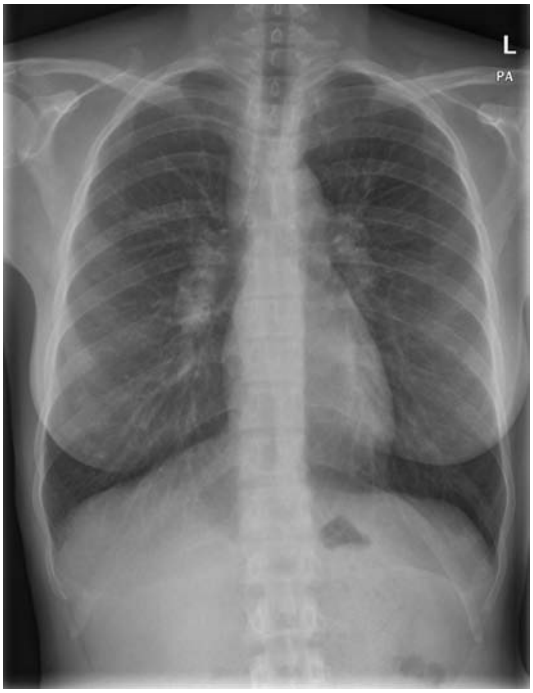


**Fig. 2.** Characteristic distribution of bilateral hilar lymphadenopathy in stage I sarcoidosis on a chest radiograph.

The groups of Niimi and colleagues[22] and Patil and colleagues[21] demonstrated that the most commonly involved nodal stations are Naruke 4R (right lower paratracheal), Naruke 10R (right hilar), Naruke 7 (subcarinal), Naruke 5 (aortapulmonary window), Naruke 11R (right interlobular), and Naruke 11L (left interlobular), as shown in **Box 1**.[21,22]

Massive hilar and/or mediastinal lymphadenopathy is often asymptomatic but can cause fatigue, retrosternal pain, dysphagia, and even pulmonary hypertension in some patients.

The differential diagnosis of hilar and mediastinal lymphadenopathy is broad, with the major diagnostic alternatives lymphoma, metastatic disease, and infections, especially tuberculosis. An important feature of lymphadenopathy in sarcoidosis is the symmetric distribution, which is unusual in these diagnostic alternatives. Lymphadenopathy can also be seen in other interstitial lung diseases, such as (idiopathic) interstitial pneumonitis and hypersensitivity pneumonitis. In diseases

other than sarcoidosis, however, usually only 1 or 2 nodes are enlarged and their maximal short axis diameter is mostly less than 15 mm.[22] Mediastinal lymphadenopathy without hilar involvement is uncommon in sarcoidosis and a biopsy-proved diagnosis is warranted.

Lymph node calcification is visible at presentation in approximately 20% of patients, increasing to 44% during disease course.[27] The morphology of calcified lymph nodes is variable and nonspecific. Sometimes, the calcification can have an eggshell appearance.[28] Calcification of lymph nodes is linked to the duration of disease and can be seen in other granulomatous disorders, like tuberculosis or histoplasmosis, as well. When comparing calcified lymph nodes in sarcoidosis and tuberculosis, in sarcoidosis their diameter was significantly larger, calcium deposition more focal, and hilar distribution more bilaterally (65% vs 8%).[23]

## PARENCHYMAL INVOLVEMENT

The HRCT appearance of pulmonary sarcoidosis has a great variability and is notorious for mimicking many other interstitial lung diseases. The most important 2 radiological patterns in sarcoidosis with involvement of the lung parenchyma are the nodular pattern and the reticulonodular pattern. The distribution of nodules on HRCT can follow 3 different patterns: random distribution, centrilobular distribution, and perilymphatic distribution.

### *Nodular and Reticulonodular Pattern*

The nodular pattern is seen in approximately 90% of sarcoidosis patients with parenchymal involvement.[29,30] Sarcoid granulomas are microscopic in size but can aggregate to form small nodules that can be seen on HRCT. These small nodules are 1 to 10 mm in diameter, usually have irregular margins, and are predominantly present in the mid and upper zones of the lungs. The nodules are frequently found along the bronchovascular bundles and in the subpleural region after a perilymphatic distribution. Aggregated subpleural nodules account for the fissural thickening that can be seen on HRCT. The nodules adjacent to interfaces of vessels, airways, and septa give these structures an irregular or beaded appearance, implicating them as pathognomic for sarcoidosis (**Fig. 3**). This pattern is also seen in histologic specimens, where granulomas are found in association with lymphatics along vessels and airways and in the subpleural area.[31] This distribution of granulomas can also explain the high rate of success in diagnosing sarcoidosis by bronchial and transbronchial biopsy. Frequently, sarcoidosis causes nodular septal thickening defining the reticulonodular pattern. A reticular pattern is a descriptive term (*reticulum* means network) with several morphologic variations ranging from generalized thickening of interlobular septa to honeycomb lung destruction. A pure reticular pattern is rarely seen in sarcoidosis.[32]


**Fig. 3.** HRCT with the classic perilymphatic distribution of nodules in a patient with sarcoidosis. Note the occurrence of small nodules along subpleural surface and fissures, along interlobular septa and the peribronchovascular bundles, giving these structures a beaded appearance. This is thought pathognomic for sarcoidosis.

### *Large Nodules and Alveolar Sarcoidosis*

Sarcoid nodules can aggregate into pulmonary nodules (not >3 cm in diameter) or large masses. Such a presentation is uncommon in sarcoidosis and estimated as 2.4% to 4%.[17,25,33–35] In a retrospective analysis of African American patients, 82% had multiple masses/nodules and only 18% had a solitary lesion.[36] An air bronchogram was seen in 58% of the cases and the nodules tended to be more peripheral. The margins of the nodules are often irregular and hazy.[34] The nodules can remain stable for years; however, partial or complete regression has been described.[33] Cavitation is rarely seen in large pulmonary masses and is usually benign; however, hemoptysis can occur.[37,38] In approximately 10% to 20% of patients, massive consolidation with air bronchograms develops (**Fig. 4**).[39–42] The pathologic mechanism is loss of alveolar air due to compression of the alveoli by coalescent granulomas in the interstitium.[24] The alveolar opacities are usually present in the peripheral middle zones of the lung.[24,34]

### *Galaxy Sign, Cluster Sign, and (Reversed) Halo Sign*

Recently, 3 CT signs have been reviewed in sarcoidosis involving a more atypical distribution

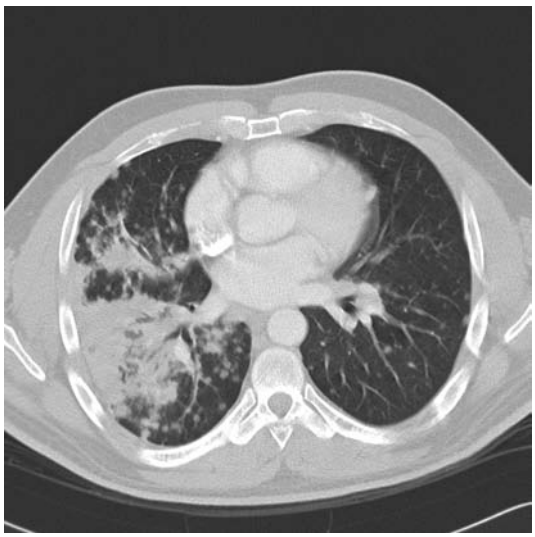

**Fig. 4.** Alveolar consolidation in the middle and right lower lobe of a sarcoidosis patient. Note the presence of air bronchograms in the major consolidation in the right lower lobe. Furthermore, multiple nodules with a mildly irregular outline are seen bilaterally.

of large and small nodules.[43] The sarcoid galaxy sign represents a large pulmonary nodule or mass surrounded by many small satellite nodules (Fig. 5). It is named after a galaxy where the stars are more concentrated to the galactic center than in the periphery. The sarcoid cluster sign is also characterized by clusters of multiple small nodules forming a pulmonary mass but, in contrast to the galaxy sign, the nodules do not tend to coalesce in the center (Fig. 6). The most important differential diagnosis for sarcoid galaxy sign or sarcoid cluster sign is tuberculosis. Clusters of small nodules can also be seen, however, in cryptococcus infection and silicosis.[43] The reversed halo sign is a far more nonspecific sign and describes a focal area of ground glass opacity surrounded by an almost complete ring of consolidation (Fig. 7). It was first described as a specific finding in patients with cryptogenic organizing pneumonia.[44] Later, several investigators described the reversed halo sign in various diseases, such as tuberculosis, aspergillosis, Wegener granulomatosis, and adenocarcinoma in situ (formerly known as bronchoalveolar carcinoma).[45] The reversed halo sign is also known as the atoll sign due to its resemblance of a ring-shaped coral reef that encloses a lagoon with shallow water.[46] A true halo sign, describing a pulmonary mass with a surrounding area of ground glass, has been rarely described in sarcoidosis.[47]

### *Ground Glass Opacities*

Ground glass attenuation in HRCT is defined as areas of hazy increased attenuation with preservation of bronchial and vascular margins. In sarcoidosis patients, the prevalence of ground glass opacities is estimated at 40%, ranging from 16% to 83%.[27,39,42,48,49] Historically, it was believed to represent active alveolitis but now it is thought caused by small interstitial granulomas or fibrotic

**Fig. 5.** Pulmonary mass with sarcoid galaxy sign in both left and right upper lobes in a 28-year-old sarcoidosis patient. In both upper lobes the mass is surrounded by multiple small satellite nodules.

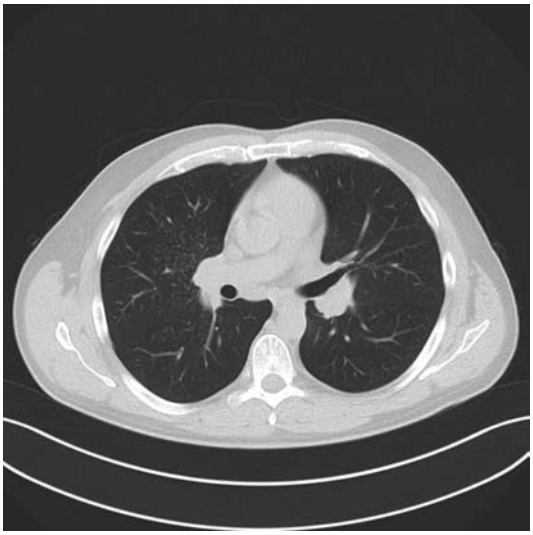

**Fig. 6.** Sarcoid cluster sign in sarcoidosis. Note the subtle clustering of micronodules without confluence in the right parahilar region.

**Fig. 7.** Reversed halo sign in both lower lobes in a 32-year-old patient clinically and radiologically suspected of sarcoidosis. There is a focal area of ground glass opacity surrounded by an almost complete ring of consolidation. Lung biopsy of the mass in the right lower lobe revealed a histopathologic diagnosis of lymphocytic interstitial pneumonia.

**Fig. 8.** Pulmonary fibrosis on a chest radiograph in a 46-year-old sarcoidosis patient. Note that the hila are shifted upward.

lesions beyond the resolution of CT.[31] Ground glass is multifocal and often accompanied by subtle micronodularity.[50] Furthermore, it is most frequently seen at disease presentation.[40] The response to steroids depends on the presence of underlying fibrosis, with clearance more likely if it is of short duration.[42]

### *Fibrotic Sarcoidosis*

At presentation, approximately 5% of sarcoidosis patients have fibrotic changes on their chest radiograph.[10,11] In an estimated 10% to 20% of patients, however, fibrosis develops or becomes more prominent during disease course.[51] On the chest radiograph, linear opacities radiating laterally from the hilum into the middle and upper zones is a characteristic finding.[24] The hila are shifted upward, and vessels and fissures are distorted (**Fig. 8**).[17] Due to compensatory hyperinflation, the lower lobes are sometimes transradiant. On HRCT, fibrotic changes are represented by fibrous bands, hilar retraction, displacement of fissures, traction bronchiectasis, honeycomb cysts, bullae, and irregular reticular opacities, including intralobular lines and irregular septal thickening. Fibrosis is seen predominantly in the upper and middle lobes, in a patchy distribution. A common feature of fibrotic sarcoidosis is the presence of conglomerated masses surrounding and encompassing vessels and bronchi. It occurs in 60% of fibrotic sarcoidosis and is associated with bronchial distortion.[41]

Fibrotic cysts, bullae, traction bronchiectasis, and paracicatricial emphysema (air space enlargement and lung destruction developing adjacent to areas of pulmonary scarring) represent advanced fibrotic sarcoidosis (**Fig. 9**). Cystic abnormalities are particularly common in the upper lobes in advanced fibrotic sarcoidosis.[52] Honeycombing (subpleural clustering of cystic airspaces) is thought less common in sarcoidosis compared with other end-stage lung diseases.[53] If present, honeycomb-like cysts are most commonly found in the upper lobes but can also be seen in the lower lobes mimicking idiopathic pulmonary fibrosis.[32]

### *Mosaic Attenuation Pattern and Air Trapping*

Mosaic attenuation is defined as a patchwork of regions with varied attenuation on HRCT. This pattern can represent patchy interstitial disease, vascular disease, or small airway disease. In patients with sarcoidosis, the presence of mosaic attenuation frequently results from small airway involvement by granulomas or fibrosis.[54,55] To verify that mosaic attenuation is caused by small airway disease, inspiratory images on CT must be compared with the parenchymal appearance on expiratory images to identify air trapping. Air trapping is a common but nonspecific feature of pulmonary sarcoidosis.[54,56]

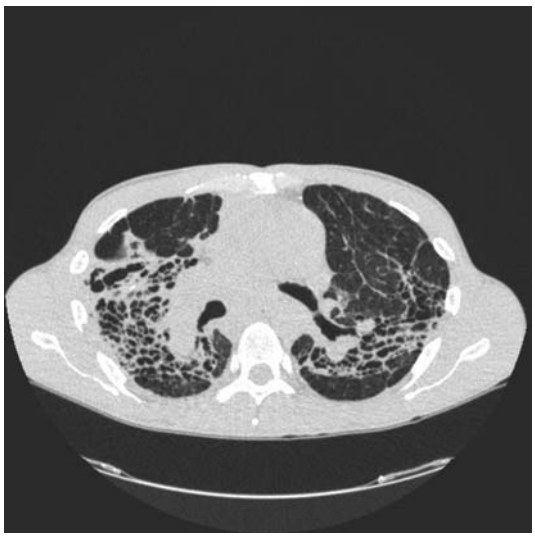

**Fig. 9.** Fibrotic pulmonary sarcoidosis on HRCT. The CT demonstrates parenchymal distortion and destruction. Multiple honeycomb cysts are noted throughout the upper lobes bilaterally.

## MYCETOMAS

The formation of mycetomas occurs in approximately 2% of sarcoidosis patients, especially in stage IV cystic disease.[57] Fungal balls can develop in preexisting bullae or cysts that are colonized by fungi, usually *Aspergillus* species. The characteristic appearance of a pulmonary aspergilloma consists of a mobile opacity occupying part or most of the cavity. It is surrounded by a peripheral rim of air known as the air crescent sign or Monod sign (**Fig. 10**).[58] A common symptom in patients with aspergillomas is hemoptysis and, when massive, can be life threatening.

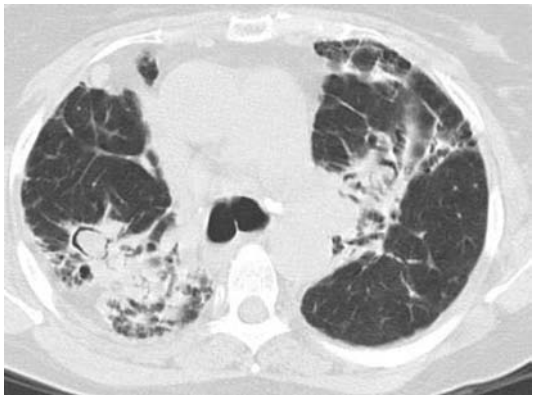

**Fig. 10.** Aspergilloma in the right upper lobe of a 57-year-old patient with advanced pulmonary sarcoidosis. The aspergilloma is surrounded by a peripheral rim of air known as the air crescent sign or Monod sign.

## PLEURAL INVOLVEMENT

### *Pleural Effusion*

In sarcoidosis, granulomas can be found on both visceral and parietal pleura. This pleural localization as well as blockage of lymphatic channels by granulomas can result in pleural effusion. Pleural effusion, however, is an uncommon manifestation of sarcoidosis with an estimated incidence of 0.7% to 10% on chest radiograph.[59–64] In a more recent study, the occurrence of pleural effusion was studied with ultrasonography in 181 patients with sarcoidosis presenting at the outpatient clinic of a university hospital.[65] In 2.8% of patients, pleural fluid was detected, with some patients having a parapneumonic effusion and congestive heart failure. Therefore, in this study only 1.1% of patients had sarcoidosis-related pleural effusion demonstrated by biopsy-proved sarcoid pleural involvement. Sarcoidosis-related pleural effusion occurs more often in the right side of the lung compared with the left (45% vs 33%, respectively).[64] It mostly resolves spontaneously within 6 months, sometimes leaving residual pleural thickening.[24,62,66]

### *Chylothorax*

The development of chylothorax is an exceptionally rare complication of sarcoidosis, with only a few case reports in the literature.[67–70] In 1 case report, chylothorax was the presenting feature of sarcoidosis.[68]

### *Pneumothorax*

It has been estimated that pneumothorax has 2% to 3% prevalence in sarcoidosis patients.[71,72] Cases of spontaneous pneumothorax may develop due to rupture of a subpleural bleb, particularly in patients with advanced fibrocystic disease.[64] Bilateral pneumothorax in sarcoidosis has also been reported.[73]

## NECROTIZING SARCOID GRANULOMATOSIS

Necrotizing Sarcoid Granulomatosis (NSG) is a rare entity and seen as a variant of sarcoidosis with, however, some uncertainty.[74] It is debated whether NSG is a manifestation of systemic sarcoidosis with necrotizing granulomata or a form of necrotizing angiitis with a sarcoid-like reaction.[75] NSG is defined by a granulomatous vasculitis, confluent non-necrotizing granulomas, and foci of infarct-like necrosis with variable degrees of fibrosis.[74,76] Since the first article

describing NSG in 1973, approximately 135 cases have been described.[77,78] Recently, however, an excellent review was published providing reasonable evidence that NSG is a manifestation of sarcoidosis and essentially the same as nodular sarcoidosis.[79]

## PULMONARY HYPERTENSION

It is estimated that 1% to 6% of patients with sarcoidosis have pulmonary hypertension, most patients having advanced stages on chest radiography (Scadding stages III and IV).[80,81] Fibrosis or extensive parenchymal abnormalities are not always present, however, and the absence should not exclude further evaluation for pulmonary hypertension.[82] Clinical characteristics are often atypical but some symptoms can suggest underlying pulmonary hypertension: dyspnea more severe compared with functional impairment, chest pain, and near-syncope on exertion. Also, approximately 25% of sarcoidosis patients with pulmonary hypertension present with signs of right-sided heart failure.[81,82] Diagnosing pulmonary hypertension in sarcoidosis solely with the use of CT is difficult and merely impossible. Severe pulmonary hypertension, however, is likely to be present when the diameter of the main pulmonary artery at the level of its bifurcation is greater than that of the adjacent ascending aorta or more than 29 mm.[83] In a study by Nunes and colleagues,[82] a higher frequency of ground glass attenuation and septal lines was found in sarcoidosis patients with pulmonary hypertension compared with sarcoidosis patients without pulmonary hypertension.

## FLUORODEOXYGLUCOSE F 18 PET/COMPUTED TOMOGRAPHY

### *Fluorodeoxyglucose F 18 Uptake in Sarcoidosis*

FDG PET/CT is widely used in oncology. FDG is a glucose analogue that is transported through the cell membrane. Once in the cytosol, FDG is phosphorylated by hexokinase and metabolically trapped as FDG-6-phosphate. After annihilation, 2 gamma photons of 511 keV each are detected by the PET camera. The current resolution of PET cameras is up to 5 mm. FDG is a well-studied and practical tracer with various applications in medicine, without the need for an onsite cyclotron.

In sarcoidosis, the granuloma contains activated macrophages and $CD4^+$ T lymphocytes. Like malignant cells, macrophages and lymphocytes express glucose transporters (GLUTs), specifically GLUT-1 and GLUT-3.[84] Analogous to glucose, FDG is transported into macrophages and activated leucocytes through GLUT-1 and GLUT-3. Therefore, FDG PET can be used in leukocyte-mediated processes, like sarcoidosis and other granulomatous diseases.[85] Lewis and Salama[86] were the first to report the use of FDG PET in sarcoidosis, and since then several important clinical studies have been performed.

The maximum standardized uptake value ($SUV_{max}$) represents the maximum amount of glucose, that is, activity, in 1 pixel. $SUV_{max}$ has proved a powerful tool in oncology because it correlates with survival and can be used for treatment monitoring. In sarcoidosis, the $SUV_{max}$ could be helpful for response assessment and correlates with recurrence. In contrast with tumors, however, sarcoidosis cannot be well demarcated and might diffusely affect organs. Therefore, the maximum activity in 1 pixel might be less appropriate.

### *Patient Preparation and Fluorodeoxyglucose F 18 PET/Computed Tomography Acquisition in Sarcoidosis*

Prior to FDG injection, patients need to fast for 6 hours. In sarcoidosis, this fasting period is preceded by a carbohydrate-restricted diet for at least 24 hours. To reduce the radiation dose and accelerate FDG excretion by the kidneys, 20 mg of furosemide is injected intravenously. Subsequently, FDG is administered when the blood glucose level is less than 7 mmol/L. The dosage of FDG is based on a patient's body weight with a minimum of 37 MBq (Mega Becquerel) and a maximum of 400 MBq; 60 minutes after FDG administration, low-dose CT is performed from the subinguinal region to the head. Low-dose CT is used for attenuation correction and optimizing image interpretation. The emission scan is performed from the subinguinal region to the head and starts 55 to 65 minutes after FDG injection. The acquisition time is 2.5 minutes per bed position. Reconstruction of the PET images is performed in accordance with the 3D–row action maximum likelihood algorithm protocol (RAMLA), applying 4 iterations with a $144 \times 144$ matrix.

Mammalian metabolism depends on glucose and fatty acids.[87] Therefore, FDG uptake in the myocardium is simply a physiologic process. The physiologic FDG uptake can be reduced by the use of unfractioned heparin, prolonged fasting period, or a carbohydrate-restricted diet for at least 24 hours prior to acquisition.[88–93] The latter has proved the most effective method. Fat and proteins are allowed, whereas all carbohydrates,

including fruit and vegetables, should be avoided. When carbohydrates are restricted, fatty acids are used and physiologic FDG uptake is absent. If so, only metabolic active processes, like granulomas, become evident. This is the basis of imaging active cardiac sarcoidosis with FDG PET/CT.

### *Radiation Dose of Fluorodeoxyglucose F 18 PET/Computed Tomography*

The radiation dose of FDG is approximately 5.8 mSv for the first-generation PET cameras, without CT scan. Over time, the cameras have become more sensitive and, in the current PET/CT systems, the FDG dosage can be reduced. The dosage is based on a patient's body weight, in accordance with European guidelines.[94] A patient with a bodyweight of 80 kg receives a radiation dose of 3.8 mSv. Disease location is more accurate because of the concurrently obtained CT, also performed for attenuation correction. The low-dose CT adds approximately 2.9 mSv to the radiation dose. Therefore, the radiation dose of FDG PET/CT from the head to the subinguinal regions is approximately 6.7 mSv.

Although FDG PET/CT is a noninvasive technique, it should be performed with care. FDG PET/CT is more expensive than other tests or techniques and radiation exposure should be taken into account. Frequent, repetitive FDG PET/CT is, therefore, not recommended.

## CHEST RADIOGRAPH AND FLUORODEOXYGLUCOSE F 18 PET/COMPUTED TOMOGRAPHY

Chest radiography is commonly performed at the initial presentation of sarcoidosis. It is cheap and widely available and in 85% to 95% of patients abnormal findings are present.[95]

Staging of pulmonary disease is based on the Scadding criteria for chest radiography. It describes the presence of bilateral hilar adenopathy, parenchymal involvement, and signs of fibrosis.[4,96,97] Although the staging system provides prognostic information, differentiating between active inflammation, fibrosis, and inactive disease is difficult. The Scadding stages do not correlate with disease activity imaged by FDG PET/CT.[98,99] Patients with stage 0 and stage IV disease frequently demonstrate disease activity in hila and/or lung parenchyma. Additionally, a majority of patients with stage I show active parenchymal disease. These data suggest that FDG PET/CT is more accurate than chest radiography in the evaluation of active parenchymal and/or lymph node involvement of sarcoidosis.

## HIGH-RESOLUTION COMPUTED TOMOGRAPHY AND FLUORODEOXYGLUCOSE F 18 PET/COMPUTED TOMOGRAPHY

HRCT is able to assess the lung parenchyma meticulously due to its high spatial resolution. It is, therefore, superior to conventional radiography in detecting parenchymal distortion, nodules, and early fibrosis. Volumetric scanning with multidetector CT scans has become routine in most institutions and enables imaging of the whole lung in 1 single breath-hold.[98] It has become a powerful technique in the diagnosis of diffuse parenchymal lung disease. Compared with conventional chest radiography, HRCT is more accurate in diagnosing sarcoidosis and has a better interobserver agreement.[48]

The prognostic value of HRCT has been studied by evaluating serial HRCT scans. Architectural distortion, traction bronchiectasis, cysts, and honeycombing are irreversible but nodular disease is reversible in most patients. Ground glass, interlobular septal thickening, and irregular linear opacities, however, may or may not be reversible and can progress to fibrosis.[11,42,100–104]

In stage I sarcoidosis, no predictive value of parenchymal opacities in HRCT could be found during 2-year follow-up.[105]

Only a few studies have compared FDG PET/CT and HRCT. Ambrosini and colleagues[106] evaluated 35 scans in a heterogeneous group of 28 patients. FDG PET/CT was indicated for staging, assessment of disease activity, evaluation of disease activity during or after therapy, suspicion of cardiac sarcoidosis, or follow-up. Active disease at FDG PET/CT was defined by any pathologic FDG uptake. Their HRCT criteria for active disease were enlarged lymph nodes with or without calcifications, large or small nodules with perilymphatic distribution, diffuse or random distribution of nodules, consolidation or ground glass density, cluster sign, galaxy sign, halo sign, atoll sign, or airways abnormalities with or without air trapping on expiration. Active disease was present in 24 FDG PET/CT scans (69%) and 25 HRCT scans (71%). Only 10 scans, however, demonstrated corresponding active disease in the overall concordant group of 16.

Using a semiquantitative HRCT scoring system, Mostard and colleagues[107] compared HRCT and FDG PET in 95 sarcoidosis patients. HRCT features associated with increased FDG uptake are parenchymal consolidations in 48%, lymph nodes in 25%, intraparenchymal nodules in 21%, septal and nonseptal lines in 4%, and pleural thickening in 2%.

Signs of fibrosis on HRCT regularly show metabolic active lung parenchyma on FDG PET/CT. Although the amount of uptake is variable in fibrotic sarcoidosis, it is much higher than in idiopathic pulmonary fibrosis.[108] The significantly higher metabolism in sarcoidosis is suggested to reflect granulomatous inflammation, whereas the slightly increased FDG activity in idiopathic pulmonary fibrosis might be the result of increased glucose metabolism in fibroblasts. Because fibrotic changes on HRCT may vary in FDG activity, it seems that HRCT is not able to distinguish active, ongoing fibrogenesis and inactive, end-stage fibrosis.[2,83]

### *Pulmonary Function and Fluorodeoxyglucose F 18 PET/Computed Tomography*

FDG PET/CT is able to demonstrate ongoing granulomatous inflammation in the lungs of patients with pulmonary sarcoidosis, representing active disease. Keijsers and colleagues[109] correlated baseline FDG PET with changes in vital capacity (VC), forced expiratory volume in the first second of expiration ($FEV_1$), and diffusion capacity of lung for carbon monoxide (DLCO) after 1 year in 43 newly diagnosed sarcoidosis patient. There was significant improvement of VC, $FEV_1$, and DLCO in patients with diffuse lung parenchymal activity receiving immunosuppressive therapy (n = 16). Patients with diffuse lung parenchymal activity without therapy (n = 11) showed a significant decrease in DLCO. On the other hand, there was no change in VC, $FEV_1$, and DLCO in patients without lung parenchymal activity and without treatment. In addition, the change in metabolic activity imaged by FDG PET was evaluated in 11 patients treated with infliximab and compared with pulmonary function tests.[110] Clinical improvement was associated with an overall reduced metabolic activity. In particular, the decrease in metabolic activity of the lung parenchyma, expressed as $SUV_{max}$, showed a significant correlation with the increase in VC (**Fig. 11**). These results suggest that the extent of active disease reflects the potential functional improvement that can be achieved and that lung parenchymal metabolic activity may have prognostic value.

From the authors' experience, the absence of FDG uptake in the lungs of patients with prolonged parenchymal sarcoidosis does indicate little or no lung functional improvement after initiation or intensification of immunosuppressive treatment (**Fig. 12**).

### *Fluorodeoxyglucose F 18 PET/Computed Tomography in Cardiac Sarcoidosis*

Cardiac involvement in sarcoidosis may occur at any time and even without pulmonary or other systemic disease. Cardiac sarcoidosis may have major clinical consequences given the potential conduction defects and lethal arrhythmias. Accurate diagnosis of cardiac sarcoidosis is, therefore, of great importance.

Sarcoidosis can affect the pericardium, myocardium, and endocardium. Myocardial involvement is predominantly in the left ventricular wall followed by the papillary muscles, the interventricular septum, the right ventricular wall, and the atria.[111,112] The guidelines of the Japanese Ministry of Health and Welfare for the diagnosis of cardiac sarcoidosis are updated but FDG PET/CT is not included in the work-up.[113] FDG PET/CT has, however, been shown a promising tool to evaluate cardiac involvement[114] (**Fig. 13**).

Focal FDG uptake strongly suggests cardiac involvement, although a diffuse pattern may be seen as well.[89,90] Sensitivity of FDG PET in the diagnosis of cardiac sarcoidosis has been reported as high. A meta-analysis showed a pooled sensitivity of 89% and specificity of 78%.[115] A study comparing cardiac magnetic resonance (CMR) and FDG PET demonstrated a favorable sensitivity over MRI of 87.5% versus 75%, respectively.[114] On the other hand, Mehta and colleagues[116] found a higher sensitivity for FDG PET compared with MRI (86% vs 36%, respectively). Both MRI and PET scanning may be indicated in patients in whom the diagnosis of cardiac sarcoidosis is uncertain.[117]

Blankstein and colleagues[118] performed cardiac PET/CT in 118 patients with cardiac sarcoidosis. FDG PET/CT was performed to evaluate the presence of active inflammation. Rubidium Rb 82 PET/CT was carried out to assess perfusion defects and caused scarring. Patients were categorized by perfusion and/or metabolism abnormalities and outcome was measured; 47 patients had a normal and 71 had an abnormal cardiac PET. The presence of perfusion defects combined with increased metabolism was predictive of death or sustained ventricular tachycardia with a hazard ratio of 3.9.

In addition, an abnormal FDG PET scan is associated with an increased risk of major cardiac events.[118] Japanese criteria demonstrated poor sensitivity and had no significant association with adverse events, suggesting an important added value of FDG PET beyond the Japanese guidelines. In cardiac sarcoidosis patients with implantable cardioverter-defibrillators (ICDs), positive FDG PET scans for cardiac sarcoidosis in combination with positive MRI predicted a higher ventricular tachycardia and ventricular fibrillation risk than positive MRI alone.[119] Remarkably, 90% of FDG PET scans were positive versus 67% positive

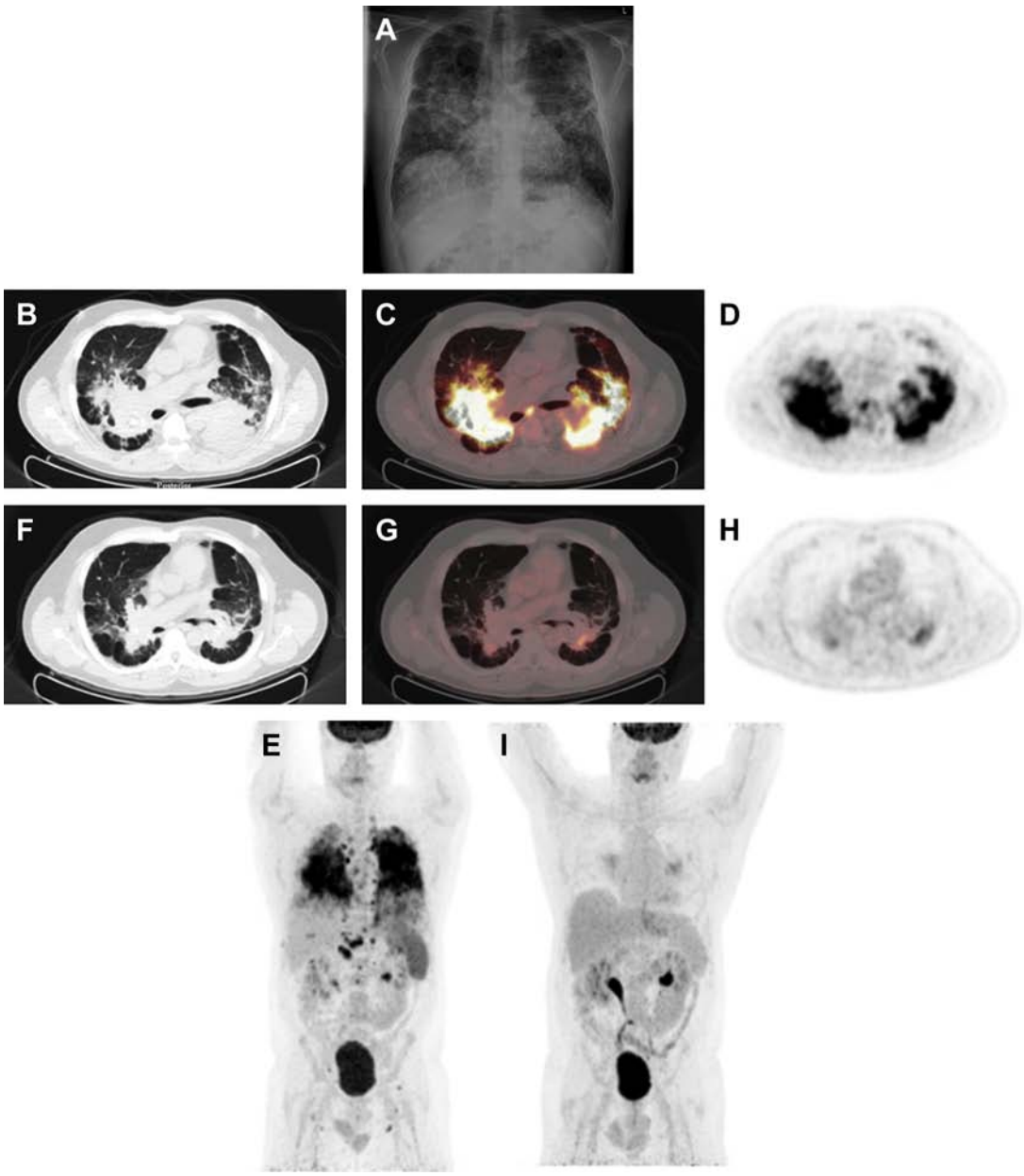


**Fig. 11.** A 51-year-old male patient was diagnosed with sarcoidosis 6 years prior to presentation at St. Antonius Hospital (The Netherlands). Initially, he was treated with prednisone, followed by methotrexate because of progressive dyspnea with pulmonary deterioration. With methotrexate, PFT remained decreased, but stable (VC 62% predicted, $FEV_1$ 30% predicted, and DLCO 40% predicted). Chest radiography after 6 months demonstrated unchanged pulmonary infiltrates with signs of fibrosis (*A*). ACE was 85 U/L (normal 14–62 U/L) and sIL-2R was 10.500 pg/mL (normal <3000 pg/mL). FDG PET/CT was performed to evaluate the inflammation in the lung parenchyma. Widespread active disease was demonstrated in the lung parenchyma with active lymph nodes in the hila, mediastinum, abdomen, and inguinal regions (*B–E*). In addition, an active spleen was present. Infliximab was started and after 6 months, the fatigue and dyspnea were decreased. PFT was improved (VC 76% predicted, $FEV_1$ 38% predicted, and DLCO 50% predicted), ACE remained unchanged, but sIL-2R dropped to 3814 pg/mL. FDG PET/CT showed a slight remaining metabolic activity in the perihilar regions (*F–I*). ACE, angiotensin converting enzyme; PFT, pulmonary function test; sIL-2R, soluble Interleukin-2 Receptor.

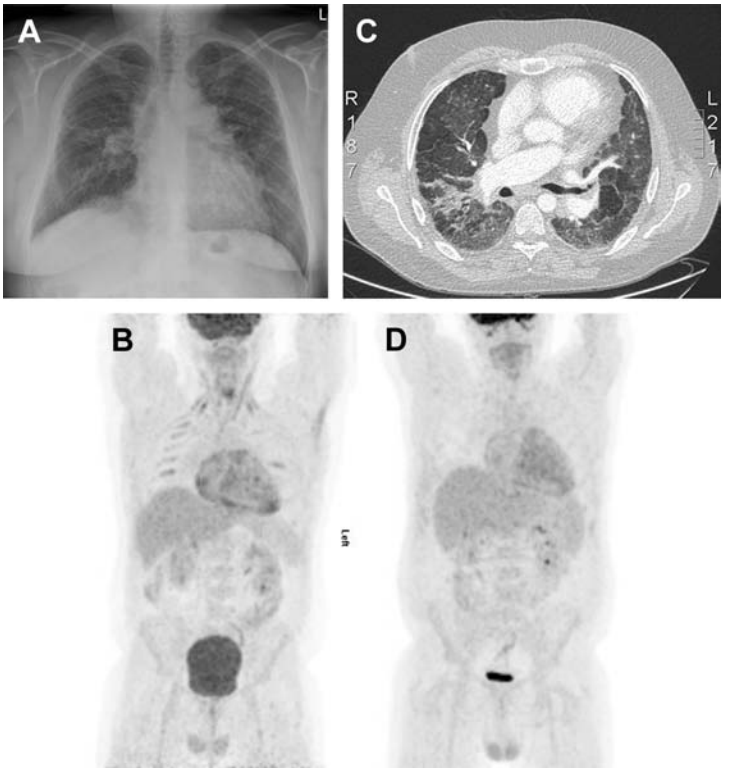


**Fig. 12.** A 39-year-old male patient was referred to St. Antonius Hospital (The Netherlands) because of pulmonary hypertension. He was diagnosed with sarcoidosis 2 years earlier and initially he was treated with prednisone followed by methotrexate. (*A*) Chest radiography showed mediastinal and hilar adenopathy with interstitial involvement. CMR showed a large right ventricle with signs of pulmonary hypertension but no cardiac sarcoidosis. Silfadenil was started but without improvement. PFT was invariably decreased (VC 61% predicted, $FEV_1$ 50% predicted, and DLCO 29% predicted). ACE was 50 U/L (24–82 U/L) and sIL-2R was 3538 pg/mL (normal <3000 pg/mL). (*B*) FDG PET/CT was performed to evaluate the inflammation in the lung parenchyma, but no active disease was present. The metabolic active right atrial and ventricle wall are due to the increased right ventricular pressure overload. (*C*) HRCT demonstrated mediastinal and hilar lymphnodes, traction bronchiectasis, and expanding areas of ground glass. Infliximab was started and after 6 cycles; ACE was 61 U/L and sIL-2R 4328 pg/mL. HRCT was unchanged and PFT was not improved (VC 60% predicted, $FEV_1$ 44% predicted, and DLCO 24% predicted). (*D*) FDG PET/CT was again normal. The results in this patient might indicate that the effect of immunosuppressive drugs is limited when active disease imaged by FDG PET/CT is absent. ACE, angiotensin converting enzyme; PFT, pulmonary function test; sIL-2R, soluble Interleukin-2 Receptor.

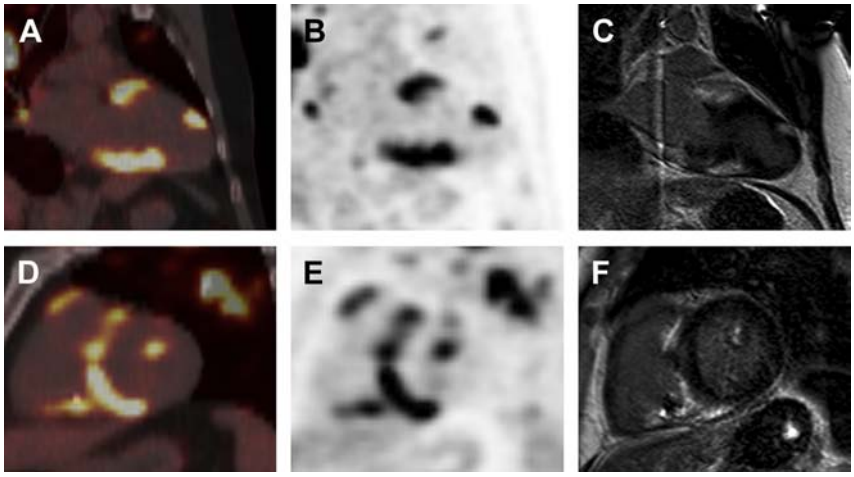


**Fig. 13.** A 47-year-old male patient presented with palpitations, an atrioventricular conduction block, and a right bundle branch block. He received a DDD pacemaker, compatible for MRI. Chest radiography after implantation showed hilar adenopathy and patchy consolidations, suspicious for sarcoidosis. During cardiac analysis at St. Antonius Hospital (The Netherlands), ventricular tachycardia occurred. FDG PET/CT ([*A* and *B*] long axis, [*D* and *E*] short axis) and CMR ([*C*] long axis, [*F*] short axis) demonstrates metabolic activity and corresponding enhancement in the right ventricle and right side of the interventricular septum and spread through the left ventricle. The left ventricular ejection fraction was 53%. The pacemaker was replaced by an ICD and prednisone was started.

MRI scans in the ICD treated group. Therefore, FDG PET seems particularly useful in patients with pacemakers or ICD or patients who cannot be evaluated with an MRI.[120]

Finally, follow-up studies demonstrated that FDG PET can detect changes in cardiac activity on treatment with corticosteroids 70.[121] This makes FDG PET useful for monitoring the effects of treatment in cardiac sarcoidosis patients.[119,122–124]

A recent consensus statement by the Heart Rhythm Society was published on the work-up in cardiac sarcoidosis.[125] In patients without symptoms and normal electrocardiogram and echocardiogram, the likelihood of cardiac involvement is low and additional testing is not recommended. In patients with 1 or more abnormalities, advanced cardiac imaging (ie, CMR and/or FDG PET/CT) can be useful.

### *When Should Fluorodeoxyglucose F 18 PET/Computed Tomography Be Used in Thoracic Sarcoidosis?*

Besides conventional markers and imaging modalities used in the treatment of thoracic sarcoidosis, there is an emerging role of FDG PET/CT. From the current literature and the authors' experience, it can be suggested to use FDG PET/CT in the following situations:

- FDG PET/CT can guide in finding occult organ localizations when histologic proof is needed. Biopsy from metabolic active lesions is more likely to yield the diagnosis than biopsy from inactive lesions.
- In patients with persistent symptoms but without signs of disease activity based on conventional markers, FDG PET/CT is able to demonstrate ongoing disease activity. Mostard and colleagues[98] evaluated FDG PET/CT in 89 patients with unexplained persistent and disabling symptoms. They found metabolic active disease in 73% with normal serum markers in 20% of these patients.
- In patients suspected of having cardiac sarcoidosis, CMR is able to detect cardiac involvement and might give rise to the implantation of a cardiac defibrillator. FDG PET/CT, on the other hand, reveals the presence of active lesions in the myocardium, which helps indicating whether immunosuppressive treatment should be started or adjusted.
- In patients with prolonged and symptomatic pulmonary sarcoidosis with fibrosis, it can be difficult to determine the presence of ongoing parenchymal disease activity. When active pulmonary sarcoidosis is still present, immunosuppressive treatment might be started or adjusted. In 14 of 15 patients with stage IV disease, FDG PET/CT revealed persistent parenchymal disease activity.[98] In addition, patients with active metabolic parenchymal disease show a significant increase of their pulmonary function after treatment. Therefore, FDG PET/CT can be used to predict the potential functional improvement that can be achieved, even in patients with stage IV disease.

## SUMMARY

Pulmonary sarcoidosis has a great variability and is notorious for mimicking many other interstitial lung diseases. Knowledge of pulmonary manifestations is important in diagnosing sarcoidosis because more than 90% of patients present with thoracic involvement. Both HRCT and FDG PET/CT are essential modalities in diagnosing and evaluation of pulmonary sarcoidosis. In addition, FDG PET/CT demonstrates extra pulmonary disease most accurate and has an important role in cardiac sarcoidosis.

## REFERENCES


1. Lynch JP 3rd, Kazerooni EA, Gay SE. Pulmonary sarcoidosis. Clin Chest Med 1997;18(4):755–85.
2. Keijsers RG, van den Heuvel DA, Grutters JC. Imaging the inflammatory activity of sarcoidosis. Eur Respir J 2013;41(3):743–51.
3. DeRemee RA. The roentgenographic staging of sarcoidosis. Historic and contemporary perspectives. Chest 1983;83(1):128–33.
4. SCADDING JG. Prognosis of intrathoracic sarcoidosis in England. A review of 136 cases after five years' observation. Br Med J 1961;2(5261):1165–72.
5. Van den Heuvel DA, de Jong PA, Zanen P, et al. Chest computed tomography-based scoring of thoracic sarcoidosis: inter-rater reliability of CT abnormalities. Eur Radiol 2015;25(9):2558–66.
6. Drent M, de Vries J, Lenters M, et al. Sarcoidosis: assessment of disease severity using HRCT. Eur Radiol 2003;13(11):2462–71.
7. Veltkamp M, van Moorsel CH, Rijkers GT, et al. Genetic variation in the Toll-like receptor gene cluster (TLR10-TLR1-TLR6) influences disease course in sarcoidosis. Tissue Antigens 2012;79(1):25–32.
8. Hillerdal G, Nou E, Osterman K, et al. Sarcoidosis: epidemiology and prognosis. A 15-year European study. Am Rev Respir Dis 1984;130(1):29–32.
9. Statement on sarcoidosis. Joint statement of the American thoracic society (ATS), the European Respiratory Society (ERS) and the World

Association of Sarcoidosis and Other Granulomatous Disorders (WASOG) adopted by the ATS Board of Directors and by the ERS Executive Committee, February 1999. Am J Respir Crit Care Med 1999;160(2):736–55.
10. Baughman RP, Teirstein AS, Judson MA, et al. Clinical characteristics of patients in a case control study of sarcoidosis. Am J Respir Crit Care Med 2001;164(10 Pt 1):1885–9.
11. Nunes H, Brillet PY, Valeyre D, et al. Imaging in sarcoidosis. Semin Respir Crit Care Med 2007; 28(1):102–20.
12. Baughman RP, Lower EE, Tami T. Upper airway. 4: sarcoidosis of the upper respiratory tract (SURT). Thorax 2010;65(2):181–6.
13. James DG, Barter S, Jash D, et al. Sarcoidosis of the upper respiratory tract (SURT). J Laryngol Otol 1982;96(8):711–8.
14. Panselinas E, Halstead L, Schlosser RJ, et al. Clinical manifestations, radiographic findings, treatment options, and outcome in sarcoidosis patients with upper respiratory tract involvement. South Med J 2010;103(9):870–5.
15. Shorr AF, Torrington KG, Hnatiuk OW. Endobronchial biopsy for sarcoidosis: a prospective study. Chest 2001;120(1):109–14.
16. Chambellan A, Turbie P, Nunes H, et al. Endoluminal stenosis of proximal bronchi in sarcoidosis: bronchoscopy, function, and evolution. Chest 2005;127(2):472–81.
17. Kirks DR, McCormick VD, Greenspan RH. Pulmonary sarcoidosis. Roentgenologic analysis of 150 patients. Am J Roentgenol Radium Ther Nucl Med 1973;117(4):777–86.
18. James DG, Neville E, Siltzbach LE. A worldwide review of sarcoidosis. Ann N Y Acad Sci 1976;278: 321–34.
19. Siltzbach LE, James DG, Neville E, et al. Course and prognosis of sarcoidosis around the world. Am J Med 1974;57(6):847–52.
20. Sider L, Horton ES Jr. Hilar and mediastinal adenopathy in sarcoidosis as detected by computed tomography. J Thorac Imaging 1990; 5(2):77–80.
21. Patil SN, Levin DL. Distribution of thoracic lymphadenopathy in sarcoidosis using computed tomography. J Thorac Imaging 1999;14(2):114–7.
22. Niimi H, Kang EY, Kwong JS, et al. CT of chronic infiltrative lung disease: prevalence of mediastinal lymphadenopathy. J Comput Assist Tomogr 1996; 20(2):305–8.
23. Gawne-Cain ML, Hansell DM. The pattern and distribution of calcified mediastinal lymph nodes in sarcoidosis and tuberculosis: a CT study. Clin Radiol 1996;51(4):263–7.
24. Rabinowitz JG, Ulreich S, Soriano C. The usual unusual manifestations of sarcoidosis and the "hilar haze"–a new diagnostic aid. Am J Roentgenol Radium Ther Nucl Med 1974;120(4):821–31.
25. Romer FK. Presentation of sarcoidosis and outcome of pulmonary changes. Dan Med Bull 1982;29(1):27–32.
26. Spann RW, Rosenow EC 3rd, DeRemee RA, et al. Unilateral hilar or paratracheal adenopathy in sarcoidosis: a study of 38 cases. Thorax 1971; 26(3):296–9.
27. Murdoch J, Muller NL. Pulmonary sarcoidosis: changes on follow-up CT examination. AJR Am J Roentgenol 1992;159(3):473–7.
28. McLoud TC, Putman CE, Pascual R. Eggshell calcification with systemic sarcoidosis. Chest 1974;66(5):515–7.
29. McLoud TC, Epler GR, Gaensler EA, et al. A radiographic classification for sarcoidosis: physiologic correlation. Invest Radiol 1982;17(2): 129–38.
30. Israel HL, Karlin P, Menduke H, et al. Factors affecting outcome of sarcoidosis. Influence of race, extrathoracic involvement, and initial radiologic lung lesions. Ann N Y Acad Sci 1986;465: 609–18.
31. Nishimura K, Itoh H, Kitaichi M, et al. Pulmonary sarcoidosis: correlation of CT and histopathologic findings. Radiology 1993;189(1):105–9.
32. Padley SP, Padhani AR, Nicholson A, et al. Pulmonary sarcoidosis mimicking cryptogenic fibrosing alveolitis on CT. Clin Radiol 1996;51(11):807–10.
33. Sharma OP, Hewlett R, Gordonson J. Nodular sarcoidosis: an unusual radiographic appearance. Chest 1973;64(2):189–92.
34. Battesti JP, Saumon G, Valeyre D, et al. Pulmonary sarcoidosis with an alveolar radiographic pattern. Thorax 1982;37(6):448–52.
35. McNicol MW, Luce PJ. Sarcoidosis in a racially mixed community. J R Coll Physicians Lond 1985; 19(3):179–83.
36. Malaisamy S, Dalal B, Bimenyuy C, et al. The clinical and radiologic features of nodular pulmonary sarcoidosis. Lung 2009;187(1):9–15.
37. Edelman RR, Johnson TS, Jhaveri HS, et al. Fatal hemoptysis resulting from erosion of a pulmonary artery in cavitary sarcoidosis. AJR Am J Roentgenol 1985;145(1):37–8.
38. Loh GA, Lettieri CJ, Shah AA. Bronchial arterial embolisation for massive haemoptysis in cavitary sarcoidosis. BMJ Case Rep 2013;2013:1–3.
39. Leung AN, Brauner MW, Caillat-Vigneron N, et al. Sarcoidosis activity: correlation of HRCT findings with those of 67Ga scanning, bronchoalveolar lavage, and serum angiotensin-converting enzyme assay. J Comput Assist Tomogr 1998;22(2):229–34.
40. Brauner MW, Grenier P, Mompoint D, et al. Pulmonary sarcoidosis: evaluation with high-resolution CT. Radiology 1989;172(2):467–71.

41. Abehsera M, Valeyre D, Grenier P, et al. Sarcoidosis with pulmonary fibrosis: CT patterns and correlation with pulmonary function. AJR Am J Roentgenol 2000;174(6):1751–7.
42. Remy-Jardin M, Giraud F, Remy J, et al. Pulmonary sarcoidosis: role of CT in the evaluation of disease activity and functional impairment and in prognosis assessment. Radiology 1994;191(3):675–80.
43. Marchiori E, Zanetti G, Barreto MM, et al. Atypical distribution of small nodules on high resolution CT studies: patterns and differentials. Respir Med 2011;105(9):1263–7.
44. Voloudaki AE, Bouros DE, Froudarakis ME, et al. Crescentic and ring-shaped opacities. CT features in two cases of bronchiolitis obliterans organizing pneumonia (BOOP). Acta Radiol 1996; 37(6):889–92.
45. Marchiori E, Zanetti G, Mano CM, et al. The reversed halo sign: another atypical manifestation of sarcoidosis. Korean J Radiol 2010;11(2): 251–2.
46. Zompatori M, Poletti V, Battista G, et al. Bronchiolitis obliterans with organizing pneumonia (BOOP), presenting as a ring-shaped opacity at HRCT (the atoll sign). A case report. Radiol Med 1999;97(4): 308–10.
47. Marten K, Rummeny EJ, Engelke C. The CT halo: a new sign in active pulmonary sarcoidosis. Br J Radiol 2004;77(924):1042–5.
48. Grenier P, Chevret S, Beigelman C, et al. Chronic diffuse infiltrative lung disease: determination of the diagnostic value of clinical data, chest radiography, and CT and Bayesian analysis. Radiology 1994;191(2):383–90.
49. Grenier P, Valeyre D, Cluzel P, et al. Chronic diffuse interstitial lung disease: diagnostic value of chest radiography and high-resolution CT. Radiology 1991;179(1):123–32.
50. Martin SG, Kronek LP, Valeyre D, et al. High-resolution computed tomography to differentiate chronic diffuse interstitial lung diseases with predominant ground-glass pattern using logical analysis of data. Eur Radiol 2010;20(6):1297–310.
51. Moller DR. Pulmonary fibrosis of sarcoidosis. New approaches, old ideas. Am J Respir Cell Mol Biol 2003;29(Suppl 3):S37–41.
52. Freundlich IM, Libshitz HI, Glassman LM, et al. Sarcoidosis. Typical and atypical thoracic manifestations and complications. Clin Radiol 1970;21(4): 376–83.
53. Primack SL, Hartman TE, Hansell DM, et al. End-stage lung disease: CT findings in 61 patients. Radiology 1993;189(3):681–6.
54. Davies CW, Tasker AD, Padley SP, et al. Air trapping in sarcoidosis on computed tomography: correlation with lung function. Clin Radiol 2000;55(3): 217–21.
55. Hansell DM, Milne DG, Wilsher ML, et al. Pulmonary sarcoidosis: morphologic associations of airflow obstruction at thin-section CT. Radiology 1998;209(3):697–704.
56. Bartz RR, Stern EJ. Airways obstruction in patients with sarcoidosis: expiratory CT scan findings. J Thorac Imaging 2000;15(4):285–9.
57. Pena TA, Soubani AO, Samavati L. Aspergillus lung disease in patients with sarcoidosis: a case series and review of the literature. Lung 2011;189(2):167–72.
58. Pesle GD, Monod O. Bronchiectasis due to aspergilloma. Dis Chest 1954;25(2):172–83.
59. Chusid EL, Siltzbach LE. Sarcoidosis of the pleura. Ann Intern Med 1974;81(2):190–4.
60. Sharma OP, Gordonson J. Pleural effusion in sarcoidosis: a report of six cases. Thorax 1975; 30(1):95–101.
61. Beekman JF, Zimmet SM, Chun BK, et al. Spectrum of pleural involvement in sarcoidosis. Arch Intern Med 1976;136(3):323–30.
62. Wilen SB, Rabinowitz JG, Ulreich S, et al. Pleural involvement in sarcoidosis. Am J Med 1974;57(2): 200–9.
63. Tommasini A, Di Vittorio G, Facchinetti F, et al. Pleural effusion in sarcoidosis: a case report. Sarcoidosis 1994;11(2):138–40.
64. Soskel NT, Sharma OP. Pleural involvement in sarcoidosis. Curr Opin Pulm Med 2000;6(5): 455–68.
65. Huggins JT, Doelken P, Sahn SA, et al. Pleural effusions in a series of 181 outpatients with sarcoidosis. Chest 2006;129(6):1599–604.
66. Littner MR, Schachter EN, Putman CE, et al. The clinical assessment of roentgenographically atypical pulmonary sarcoidosis. Am J Med 1977; 62(3):361–8.
67. Aberg H, Bah M, Waters AW. Sarcoidosis: complicated by chylothorax. Minn Med 1966;49(7): 1065–70.
68. Jarman PR, Whyte MK, Sabroe I, et al. Sarcoidosis presenting with chylothorax. Thorax 1995;50(12): 1324–5.
69. Lengyel RJ, Shanley DJ. Recurrent chylothorax associated with sarcoidosis. Hawaii Med J 1995; 54(12):817–8.
70. Parker JM, Torrington KG, Phillips YY. Sarcoidosis complicated by chylothorax. South Med J 1994; 87(8):860–2.
71. Hours S, Nunes H, Kambouchner M, et al. Pulmonary cavitary sarcoidosis: clinico-radiologic characteristics and natural history of a rare form of sarcoidosis. Medicine (Baltimore) 2008;87(3): 142–51.
72. Froudarakis ME, Bouros D, Voloudaki A, et al. Pneumothorax as a first manifestation of sarcoidosis. Chest 1997;112(1):278–80.

73. Akelsson IG, Eklund A, Skold CM, et al. Bilateral spontaneous pneumothorax and sarcoidosis. Sarcoidosis 1990;7(2):136–8.
74. Popper HH, Klemen H, Colby TV, et al. Necrotizing sarcoid granulomatosis–is it different from nodular sarcoidosis? Pneumologie 2003;57(5):268–71.
75. Koss MN, Hochholzer L, Feigin DS, et al. Necrotizing sarcoid-like granulomatosis: clinical, pathologic, and immunopathologic findings. Hum Pathol 1980;11(Suppl 5):510–9.
76. Rosen Y. Pathology of sarcoidosis. Semin Respir Crit Care Med 2007;28(1):36–52.
77. Liebow AA. The J. Burns Amberson lecture–pulmonary angiitis and granulomatosis. Am Rev Respir Dis 1973;108(1):1–18.
78. Yeboah J, Afkhami M, Lee C, et al. Necrotizing sarcoid granulomatosis. Curr Opin Pulm Med 2012;18(5):493–8.
79. Rosen Y. Four decades of necrotizing sarcoid granulomatosis: what do we know now? Arch Pathol Lab Med 2015;139(2):252–62.
80. Handa T, Nagai S, Miki S, et al. Incidence of pulmonary hypertension and its clinical relevance in patients with sarcoidosis. Chest 2006;129(5): 1246–52.
81. Sulica R, Teirstein AS, Kakarla S, et al. Distinctive clinical, radiographic, and functional characteristics of patients with sarcoidosis-related pulmonary hypertension. Chest 2005;128(3):1483–9.
82. Nunes H, Humbert M, Capron F, et al. Pulmonary hypertension associated with sarcoidosis: mechanisms, haemodynamics and prognosis. Thorax 2006;61(1):68–74.
83. Nunes H, Uzunhan Y, Freynet O, et al. Pulmonary hypertension complicating sarcoidosis. Presse Med 2012;41(6 Pt 2):e303–16.
84. Fu Y, Maianu L, Melbert BR, et al. Facilitative glucose transporter gene expression in human lymphocytes, monocytes, and macrophages: a role for GLUT isoforms 1, 3, and 5 in the immune response and foam cell formation. Blood Cells Mol Dis 2004;32(1):182–90.
85. Satomi T, Ogawa M, Mori I, et al. Comparison of contrast agents for atherosclerosis imaging using cultured macrophages: FDG versus ultrasmall superparamagnetic iron oxide. J Nucl Med 2013; 54(6):999–1004.
86. Lewis PJ, Salama A. Uptake of fluorine-18-fluorodeoxyglucose in sarcoidosis. J Nucl Med 1994;35(10):1647–9.
87. Frayn KN. The glucose-fatty acid cycle: a physiological perspective. Biochem Soc Trans 2003; 31(Pt 6):1115–9.
88. Cheng VY, Slomka PJ, Ahlen M, et al. Impact of carbohydrate restriction with and without fatty acid loading on myocardial 18F-FDG uptake during PET: a randomized controlled trial. J Nucl Cardiol 2010;17(2):286–91.
89. Ishimaru S, Tsujino I, Takei T, et al. Focal uptake on 18F-fluoro-2-deoxyglucose positron emission tomography images indicates cardiac involvement of sarcoidosis. Eur Heart J 2005;26(15):1538–43.
90. Langah R, Spicer K, Gebregziabher M, et al. Effectiveness of prolonged fasting 18f-FDG PET-CT in the detection of cardiac sarcoidosis. J Nucl Cardiol 2009;16(5):801–10.
91. Ohira H, Tsujino I, Yoshinaga K. (1)(8)F-Fluoro-2-deoxyglucose positron emission tomography in cardiac sarcoidosis. Eur J Nucl Med Mol Imaging 2011;38(9):1773–83.
92. Okumura W, Iwasaki T, Toyama T, et al. Usefulness of fasting 18F-FDG PET in identification of cardiac sarcoidosis. J Nucl Med 2004;45(12):1989–98.
93. Williams G, Kolodny GM. Suppression of myocardial 18F-FDG uptake by preparing patients with a high-fat, low-carbohydrate diet. AJR Am J Roentgenol 2008;190(2):W151–6.
94. Boellaard R, Delgado-Bolton R, Oyen WJ, et al. FDG PET/CT: EANM procedure guidelines for tumour imaging: version 2.0. Eur J Nucl Med Mol Imaging 2015;42(2):328–54.
95. Keir G, Wells AU. Assessing pulmonary disease and response to therapy: which test? Semin Respir Crit Care Med 2010;31(4):409–18.
96. Miller BH, Putman CE. The chest radiograph and sarcoidosis. Reevaluation of the chest radiograph in assessing activity of sarcoidosis: a preliminary communication. Sarcoidosis 1985;2(2):85–90.
97. Prasse A, Katic C, Germann M, et al. Phenotyping sarcoidosis from a pulmonary perspective. Am J Respir Crit Care Med 2008;177(3):330–6.
98. Mostard RL, Voo S, van Kroonenburgh MJ, et al. Inflammatory activity assessment by F18 FDG-PET/CT in persistent symptomatic sarcoidosis. Respir Med 2011;105(12):1917–24.
99. Keijsers RG, Grutters JC, van Velzen-Blad H, et al. (18)F-FDG PET patterns and BAL cell profiles in pulmonary sarcoidosis. Eur J Nucl Med Mol Imaging 2010;37(6):1181–8.
100. Akira M, Kozuka T, Inoue Y, et al. Long-term follow-up CT scan evaluation in patients with pulmonary sarcoidosis. Chest 2005;127(1):185–91.
101. Brauner MW, Lenoir S, Grenier P, et al. Pulmonary sarcoidosis: CT assessment of lesion reversibility. Radiology 1992;182(2):349–54.
102. Lynch DA, Webb WR, Gamsu G, et al. Computed tomography in pulmonary sarcoidosis. J Comput Assist Tomogr 1989;13(3):405–10.
103. Wells AU, Rubens MB, du Bois RM, et al. Functional impairment in fibrosing alveolitis: relationship to reversible disease on thin section computed tomography. Eur Respir J 1997;10(2):280–5.

104. Wells AU, Rubens MB, du Bois RM, et al. Serial CT in fibrosing alveolitis: prognostic significance of the initial pattern. AJR Am J Roentgenol 1993;161(6): 1159–65.
105. Ziora D, Kornelia K, Jastrzebski D, et al. High resolution computed tomography in 2-year follow-up of stage I sarcoidosis. Adv Exp Med Biol 2013; 788:369–74.
106. Ambrosini V, Zompatori M, Fasano L, et al. (18)F-FDG PET/CT for the assessment of disease extension and activity in patients with sarcoidosis: results of a preliminary prospective study. Clin Nucl Med 2013;38(4):e171–7.
107. Mostard RL, van Kroonenburgh MJ, Drent M. The role of the PET scan in the management of sarcoidosis. Curr Opin Pulm Med 2013;19(5):538–44.
108. Groves AM, Win T, Screaton NJ, et al. Idiopathic pulmonary fibrosis and diffuse parenchymal lung disease: implications from initial experience with 18F-FDG PET/CT. J Nucl Med 2009;50(4):538–45.
109. Keijsers RG, Verzijlbergen EJ, van den Bosch JM, et al. 18F-FDG PET as a predictor of pulmonary function in sarcoidosis. Sarcoidosis Vasc Diffuse Lung Dis 2011;28(2):123–9.
110. Keijsers RG, Verzijlbergen JF, van Diepen DM, et al. 18F-FDG PET in sarcoidosis: an observational study in 12 patients treated with infliximab. Sarcoidosis Vasc Diffuse Lung Dis 2008;25(2): 143–9.
111. Roberts WC, McAllister HA Jr, Ferrans VJ. Sarcoidosis of the heart. A clinicopathologic study of 35 necropsy patients (group 1) and review of 78 previously described necropsy patients (group 11). Am J Med 1977;63(1):86–108.
112. Tavora F, Cresswell N, Li L, et al. Comparison of necropsy findings in patients with sarcoidosis dying suddenly from cardiac sarcoidosis versus dying suddenly from other causes. Am J Cardiol 2009;104(4):571–7.
113. Watanabe E, Kimura F, Nakajima T, et al. Late gadolinium enhancement in cardiac sarcoidosis: characteristic magnetic resonance findings and relationship with left ventricular function. J Thorac Imaging 2013;28(1):60–6.
114. Ohira H, Tsujino I, Ishimaru S, et al. Myocardial imaging with 18F-fluoro-2-deoxyglucose positron emission tomography and magnetic resonance imaging in sarcoidosis. Eur J Nucl Med Mol Imaging 2008;35(5):933–41.
115. Youssef G, Leung E, Mylonas I, et al. The use of 18F-FDG PET in the diagnosis of cardiac sarcoidosis: a systematic review and metaanalysis including the Ontario experience. J Nucl Med 2012;53(2):241–8.
116. Mehta D, Lubitz SA, Frankel Z, et al. Cardiac involvement in patients with sarcoidosis: diagnostic and prognostic value of outpatient testing. Chest 2008;133(6):1426–35.
117. Skali H, Schulman AR, Dorbala S. 18F-FDG PET/CT for the assessment of myocardial sarcoidosis. Curr Cardiol Rep 2013;15(4):352.
118. Blankstein R, Osborne M, Naya M, et al. Cardiac positron emission tomography enhances prognostic assessments of patients with suspected cardiac sarcoidosis. J Am Coll Cardiol 2014;63(4): 329–36.
119. Betensky BP, Tschabrunn CM, Zado ES, et al. Long-term follow-up of patients with cardiac sarcoidosis and implantable cardioverter-defibrillators. Heart Rhythm 2012;9(6):884–91.
120. Sekhri V, Sanal S, Delorenzo LJ, et al. Cardiac sarcoidosis: a comprehensive review. Arch Med Sci 2011;7(4):546–54.
121. Soussan M, Brillet PY, Nunes H, et al. Clinical value of a high-fat and low-carbohydrate diet before FDG-PET/CT for evaluation of patients with suspected cardiac sarcoidosis. J Nucl Cardiol 2013; 20(1):120–7.
122. Gyorik S, Ceriani L, Menafoglio A, et al. 18F-FDG PET scan as follow-up tool for sarcoidosis with symptomatic cardiac conduction disturbances requiring a pacemaker. Thorax 2007;62(6):560.
123. Smedema JP, White L, Klopper AJ. FDG-PET and MIBI-Tc SPECT as follow-up tools in a patient with cardiac sarcoidosis requiring a pacemaker. Cardiovasc J Afr 2008;19(6):309–10.
124. Mc Ardle BA, Leung E, Ohira H, et al. The role of F(18)-fluorodeoxyglucose positron emission tomography in guiding diagnosis and management in patients with known or suspected cardiac sarcoidosis. J Nucl Cardiol 2013;20(2):297–306.
125. Birnie DH, Sauer WH, Bogun F, et al. HRS expert consensus statement on the diagnosis and management of arrhythmias associated with cardiac sarcoidosis. Heart Rhythm 2014;11(7):1305–23.